International Journal of Clinical Oncology (2019) 24:1020–1029
https://doi.org/10.1007/s10147-019-01451-9

ORIGINAL ARTICLE

Cell-type-specific sensitivity of bortezomib in the methotrexate-resistant primary central nervous system lymphoma cells

Azusa Hayano[1] · Yasuo Takashima[1] · Ryuya Yamanaka[1]

Received: 17 December 2018 / Accepted: 11 April 2019 / Published online: 16 April 2019

Abstract

Background Methotrexate (MTX) is used in first-line treatment of primary central nervous system lymphoma (PCNSL), but most cases result in relapse-acquired resistance to MTX. However, only few studies have reported on internal changes and chemotherapies in PCNSL.

Methods In this study, we generated two MTX-resistant PCNSL cell lines, designated MTX-HKBML and MTX-TK, in addition to a MTX-resistant Burkitt lymphoma cell line, designated MTX-RAJI. We examined gene expression changes and drug sensitivity to a proteasome inhibitor, bortezomib, in these cells.

Results Cytotoxic tests revealed that the 50% inhibitory concentration for MTX in MTX-HKBML is markedly higher than that in the other two cell lines. Expression of the genes in MTX and folate metabolisms, including gamma-glutamyl hydrolase and dihydrofolate reductase, are upregulated in both MTX-HKBML and MTX-TK, whereas the gene expression of folylpolyglutamate synthetase, thymidylate synthase, and methylenetetrahydrofolate dehydrogenase 1 were upregulated and downregulated in MTX-HKBML and MTX-TK, respectively, on the other hand, bortezomib sensitivity was observed in MTX-TK, as compared with control TK, but not in MTX-HKBML.

Conclusion These results indicate the cell-type-specific changes downstream of metabolic pathways for MTX and folate, bortezomib sensitivity, and purine and pyrimidine syntheses, in each PCNSL cell line. The MTX-resistant lymphoma cell lines established may be useful for in vitro relapse models for MTX and development of salvage chemotherapy and drug discovery.

Keywords Primary central nervous system lymphoma · Methotrexate · Bortezomib · Folate metabolism · Purine and pyrimidine syntheses

Introduction

Primary central nervous system (CNS) lymphoma (PCNSL) is a rare form of extranodal non-Hodgkin lymphoma (NHL) restricted to the CNS, which accounts for 3–5% of all primary brain tumors [1, 2]. Most of the PCNSLs are aggressive B-cell-type NHLs and are pathologically classified into a subtype of diffuse large B-cell lymphoma (DLBCL) [1, 3]. The median overall survival (OS) is improved with the high-dose methotrexate (MTX)-containing chemotherapy [4–6]. However, most of the cases result in relapse-acquired resistance to MTX with a poor prognosis [7]. Therefore, studies on relapse-acquired resistance to MTX are needed for the development of methods of salvage chemotherapy in recurrent CNS lymphomas.

MTX is an antifolate that inhibits de novo purine and thymidine biosyntheses [8]. Dihydrofolate (DHF) reductase (DHFR) converts DHF to tetrahydrofolate (THF), which is a basic form of reduced folate coenzymes in purine and thymidine synthesis [9]. The MTX resistance is intrinsic and acquired in malignant cells through certain mechanisms,

Electronic supplementary material The online version of this article (https://doi.org/10.1007/s10147-019-01451-9) contains supplementary material, which is available to authorized users.

✉ Ryuya Yamanaka
ryaman@koto.kpu-m.ac.jp

[1] Laboratory of Molecular Target Therapy for Cancer, Graduate School of Medical Science, Kyoto Prefectural University of Medicine, 465 Kajii-cho, Kawaramachi-Hirokoji, Kamigyo-ku, Kyoto 602-8566, Japan

including decreased drug transport due to gene mutations and transcription activity of the folate carrier, increased DHFR activity, decreased DHFR affinity, and decreased polyglutamination of MTX (MTX-PGs), due to decreased folylpolyglutamate synthetase (FPGS) activity and increased gamma-glutamyl hydrolase (GGH) activity [10–12]. The activities of methylenetetrahydrofolate dehydrogenase 1 (MTHFD1), serine hydroxymethyltransferase 1 (SHMT1), 5,10-methylenetetrahydrofolate reductase (MTHFR), 5-methyltetrahydrofolate-homocysteine methyltransferase (MTR), and methionine synthase reductase (MTRR) are induced by MTX exposure since these enzymes are involved in folate metabolism and/or intracellular resupply of THF [13].

Bortezomib, a 26S proteasome inhibitor, specifically inhibits the nuclear factor-kappa B (NF-κB) pathway that is constitutively active in neoplasms, thereby inhibiting tumor growth, angiogenesis, and apoptosis [14–16]. Bortezomib was first reported to improve the rate of response and OS in refractory or relapsed multiple myeloma [17]. Subsequently, in patients with refractory or relapsed mantle cell lymphoma, bortezomib treatment improved their response rate and duration [18]. Several clinical trials have reported that bortezomib enhances the effects of chemotherapy in patients with DLBCL [19–21], whereas other clinical trials show no significance for chemotherapy that includes bortezomib [22, 23].

In this study, we generated two MTX-resistant PCNSL cell lines and one MTX-resistant non-CNS lymphoma cell line. Expression changes of the genes related to the metabolisms for MTX and folate, and the cytotoxicity for bortezomib were investigated in the cells. The results suggested cell-type-specific metabolic pathways for MTX and folate with differential expression of the related genes. Moreover, sensitivity for bortezomib was increased in the MTX-resistant TK, but not in the MTX-resistant HKBML. These results would be useful for the development of salvage chemotherapy and drug discovery.

Materials and methods

Cell culture

TK cell line was obtained from JCRB Cell Bank (Osaka, Japan). HKBML and RAJI cells were obtained from RIKEN BRC Cell Bank (Ibaraki, Japan). TK and HKBML cells were derived from PCNSL. RAJI cell line was derived from Burkitt lymphoma, which is a NHL B-cell lymphoma and was used as a reference for non-CNS lymphoma. Cells were grown in RPMI-1640 (Nacalai Tesque, Inc., Kyoto, Japan) with 10% fetal bovine serum (FBS) (Biosera, MO) for TK and RAJI cells, and in Ham's F-12 (Nacalai Tesque, Inc.) with 15% FBS for HKBML cells, at 37 °C in a humidified atmosphere with 5% CO_2.

Cytotoxicity assay

MTX-resistant cell lines were maintained in drug-free medium for 1 week before use. The cells were seeded at a density of 1.5×10^4 cells per well in 96-well plates with diluted MTX (Pfizer Japan Inc., Tokyo, Japan) and bortezomib (AdooQ Bioscience, CA) and cultured for 72 h and 48 h, respectively. Ibrutinib (ChemScene, NJ), lenalidomide (AdooQ Bioscience), EPZ-6438 (Tazemetostat: MedChem Express, Osaka, Japan), and 5-azacytidine (TCI Chemicals, Tokyo, Japan) were also used for culture for 48 h. Cell viability was measured using Cell Count Reagent SF (Nacalai Tesque, Inc.). The IC_{50} value was calculated from the regression curve fit by non-linear regression analysis using the JMP 10 built-in module (SAS Institute Japan, Tokyo). Combination index (CI) of MTX and other drugs was calculated, as described [24].

Quantification of intracellular MTX

Cells were cultured in media with 5.0×10^{-8} M MTX for 4 h. Intracellular MTX concentration was measured by Nanopia e TDM Methotrexate according to the manufacturer's instruction (Sekisui Medical, Tokyo, Japan).

Quantitative polymerase chain reaction (qPCR)

Total RNAs were extracted from cells using AllPrep DNA/RNA/miRNA Universal Kit (QIAGEN GmbH, Hilden, Germany) and reverse-transcribed into cDNAs using SuperScript III First-Strand Synthesis SuperMix (Thermo Fisher Scientific, MA). qPCR was performed using Platinum SYBR Green qPCR SuperMix (Thermo Fisher Scientific) and ABI StepOne Plus real-time PCR system (Thermo Fisher Scientific). Primers used are listed in Table 1. The mRNA expression levels of genes were normalized to the values of threshold cycle (C_T) of glyceraldehyde 3-phosphate dehydrogenase (GAPDH) and the fold changes were calculated using the delta–delta C_T method [25].

Statistical analysis

Statistical analysis was performed using two-tailed Student's *t* test with JMP 10 (SAS Institute Japan). $P<0.05$ was considered statistically significant.

Table 1 List of primers used

Gene symbol	Gene name	Forward primer	Reverse primer
ATIC	5-Aminoimidazole-4-carboxamide ribonucleotide formyltransferase/IMP cyclohydrolase	GAGGGACTGCAAAAGCTCTC	GGAAATCCCGTCAACTCAGA
DHFR	Dihydrofolate reductase	CATGGTCTGGATAGTTGGTGGC	GTGTCACTTTCAAAGTCTTGCATG
FPGS	Folylpolyglutamate synthase	CCCTGCCAGTTTGACTATGC	CTGTGAAGTTCTGTTGGTCTGC
GAPDH	Glyceraldehyde-3-phosphate dehydrogenase	GCACCGTCAAGGCTGAGAAC	TGGTGAAGACGCCAGTGGA
GART	Phosphoribosylglycinamide formyltransferase, Phosphoribosylglycinamide synthetase	TCCCTGAGAAACTTGGGGTA	GCTGCAACCATGAGAAGACC
GGH	Gamma-glutamyl hydrolase	AGGCTGGATCTTACAGAGAAAGAC	CTGAGCGTCTGAGGTCAACA
MTHFD1	Methylenetetrahydrofolate dehydrogenase, cyclohydrolase and formyltetrahydrofolate synthetase 1	TTGGACAGGCTCCAACGGAGAA	AGAAGTGGTGAGAGCCAGGACA
MTHFR	Methylenetetrahydrofolate reductase	CCGGGTTAATTACCACCTTG	ATTCGGCTGCAGTTCAGG
MTR	5-Methyltetrahydrofolate-homocysteine methyltransferase	CCAACTTGTCCTTCTCCTTCCG	CATACACAGGGAGGTTTCCAGC
MTRR	5-Methyltetrahydrofolate-homocysteine methyltransferase reductase	TTCTTGCCAGCCACCACTCAGT	CAGAACCTCTGTTGTGGCAGTAG
SHMT1	Serine hydroxymethyltransferase 1	TGAACACTGCCATGTGGTGACC	CTCTTTGCCAGTCTTGGGATCC
SLC19A1	Solute carrier family 19 (folate transporter), member 1, reduced folate carrier (RFC1)	CTTTGCCACCATCGTCAAGACC	GGACAGGATCAGGAAGTACACG
TYMS	Thymidylate synthetase	CCCAGTTTATGGCTTCCAGT	GCAGTTGGTCAACTCCCTGT

GAPDH was used for normalization control

Results

Generation of MTX-resistant cells

MTX-resistant cell lines, including two PCNSL-derived cell lines, designated MTX-HKBML and MTX-TK, and a non-CNS lymphoma-derived cell line, designated MTX-RAJI, were generated from each parent cell line by continuous exposure to stepwise increasing concentrations of MTX as follows: 20–100 nM for HKBML, and 20–1000 nM for TK and RAJI, in cell culture media for 2.5–5 months. The resistance of the cells to MTX was evaluated using the ratio of 50% inhibitory concentration (IC_{50}) in MTX-resistant cells compared to that in the parent cells after treatment with various concentrations of MTX (1–10 mM) for 72 h. MTX-HKBML showed markedly high IC_{50} value for MTX (167.88 μM), compared to that in control-HKBML (0.84 μM), indicating 198.6-fold resistance to MTX in MTX-HKBML (Fig. 1a and Table 2). Similarly, MTX-TK showed higher IC_{50} value for MTX (2.15 μM), compared to that of control-TK (0.068 μM), indicating 31.6-fold resistance to MTX in MTX-TK (Fig. 1b and Table 2). MTX-RAJI also showed an increased IC_{50} value for MTX (2.43 μM), compared to that control-RAJI (0.043 μM), indicating 56.1-fold resistance to MTX in MTX-RAJI (Fig. 1c and Table 2). Simultaneously, MTX was incorporated and accumulated into MTX-HKBML (1.417-fold, $P = 0.0070$) (Fig. 1d), MTX-TK (1.674-fold, $P = 0.0062$) (Fig. 1e), and MTX-RAJI (4.639-fold, $P = 0.0014$) (Fig. 1f), compared to the control cells. These results suggest that the MTX-HKBML cell line acquired markedly strong resistance to MTX, compared to the other two cell lines.

Differential expression of genes related to MTX and folate metabolisms in MTX-resistant cells

Expression levels of eleven representative genes related to MTX and folate metabolisms in MTX-resistant cells including MTX-HKBML, MTX-TK, and MTX-RAJI were evaluated (Fig. 2). In MTX-HKBML, the expression of thymidylate synthase (TYMS) (1.83-fold), DHFR (1.66-fold), GGH (1.54-fold), FPGS (1.39-fold), aminoimidazole carboxamide ribonucleotide transformylase (ATIC) (1.34-fold), and MTHFD1 (1.25-fold) were upregulated ($P < 0.05$), whereas the expression of solute carrier family 19 (SLC19A1; also known as reduced folate carrier 1, RFC1) was decreased (0.52-fold, $P < 0.05$), compared to control-HKBML (Fig. 2a). In MTX-TK, while the expression of DHFR (1.55-fold) and GGH (1.31-fold) was upregulated, the expression levels of TYMS (0.78-fold), MTHFD1 (0.71-fold), MTHFR (0.71-fold), glycinamide ribonucleotide transformylase (GART) (0.69-fold), FPGS (0.52-fold), and SLC19A1 (0.01-fold) were downregulated, compared to control-TK ($P < 0.05$) (Fig. 2a). The expression of MTR, MTRR, and SHMT1 showed slight alterations, which were not statistically significant, in both the MTX-resistant

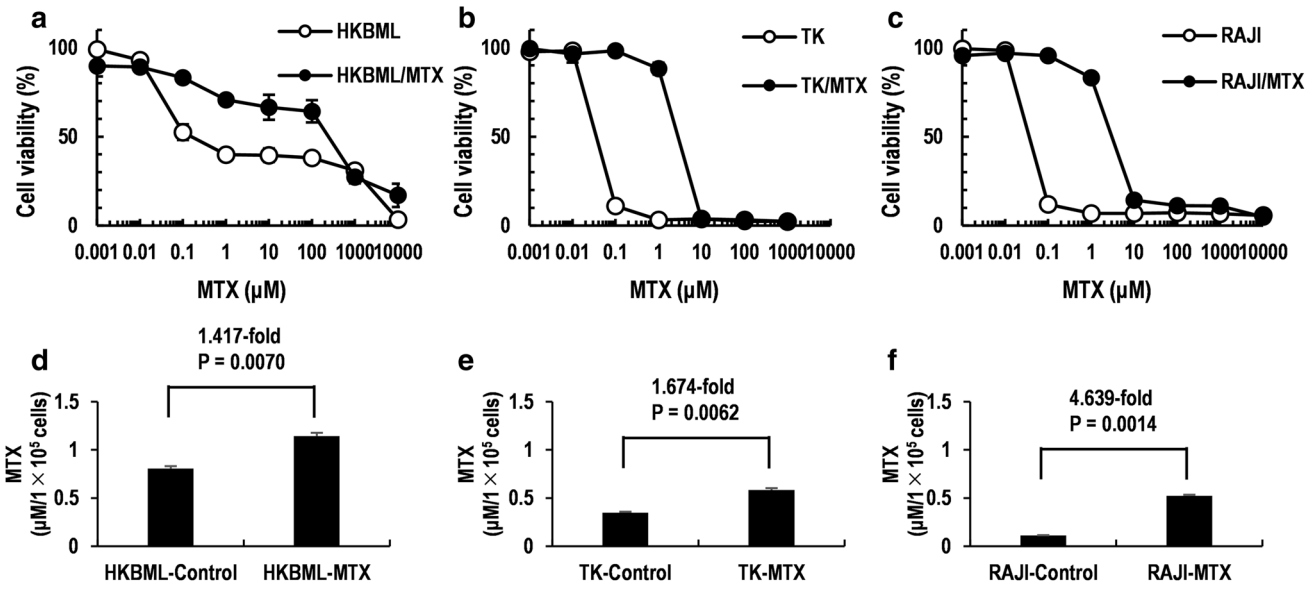

Fig. 1 Generation of the MTX-resistant cell lines. **a**–**c** Cell viability of the MTX-resistant cells. **a** MTX-resistant HKBML cells. **b** MTX-resistant TK cells. **c** MTX-resistant RAJI cells. Cell viabilities are shown. Open and closed circles indicate control and MTX-resistant cells. **d**–**f** Incorporation of MTX in the cells used. **d** HKBML and MTX-resistant HKBML cells. **e** TK and MTX-resistant TK cells. **f** RAJI and MTX-resistant RAJI cells. Cells were cultured in media with 5.0×10^{-8} mol L^{-1} (M) for 4 h. Intracellular concentration of MTX per 1×10^5 cells was measured

Table 2 The IC_{50} values of methotrexate and molecular target drugs in the MTX-resistant cells

	Methotrexate (μM)	Bortezomib (nM)	Ibrutinib (μM)	Lenalidomide (mM)	EPZ-6438 (μM)	Azacytidine (μM)
Control-HKBML	0.845	2.992	3.109	2.293	49.116	7.749
MTX-resistant HKBML	167.880	4.395	2.801	2.161	54.280	8.869
Resistance	198.609-fold	1.468-fold	0.9-fold	0.942-fold	1.105-fold	1.144-fold
Control-TK	0.068	13.521	2.355	0.899	36.898	2.067
MTX-resistant TK	2.153	4.335	2.174	1.435	29.186	0.837
Resistance (fold)	31.622-fold	0.32-fold	0.922-fold	1.596-fold	0.79-fold	0.405-fold
Control-RAJI	0.043	19.454	37.562	NA	88.980	5.473
MTX-resistant RAJI	2.427	12.942	58.314	NA	88.004	5.534
Resistance (fold)	56.104-fold	0.665-fold	1.552-fold	NA	0.989-fold	1.011-fold

IC_{50} 50% inhibitory concentration

HKBML and TK, compared to control-HKBML and TK, respectively (Fig. 2a). Basal expression levels of the almost genes examined in TK were stronger than HKBML (1.21 to 4.02-fold, $P<0.01$), except for SLC19A1 (0.94-fold, $P>0.05$) and FPGS (0.87-fold, $P>0.05$) (Fig. 2b). On the other hand, the expression levels of almost all the genes in MTX-TK were higher than those in MTX-HKBML (1.21 to 4.02-fold, $P<0.01$), except for FPGS (0.87-fold, $P>0.05$) (Fig. 2c), suggesting that TK cells possessed higher potential for MTX resistance than HKBML cells, in spite of both the cells being derived from PCNSL. To summarize the above-mentioned expression patterns of the genes, both MTX-HKBML and MTX-TK cell lines seemed to increase MTX and THF metabolism with increased expression of GGH and DHFR, respectively. Besides, both MTX-HKBML and MTX-TK seemed to dysregulate purine and pyrimidine syntheses downstream of the functions of TYMS and MTHFD1, in addition to MTX metabolism, because of abnormal expression of these genes in MTX-HKBML and MTX-TK, respectively.

In the non-CNS lymphoma RAJI with MTX resistance, although increased expression of DHFR (128.91-fold), FPGS (3.36-fold), and MTHFR (1.07-fold) was observed ($P<0.01$), almost all genes examined, including GART, MTHFD1, TYMS, SHMT1, MTR, MTRR, AITC, GGH, and SLC19A1, were decreased (0.69- to 0.92-fold,

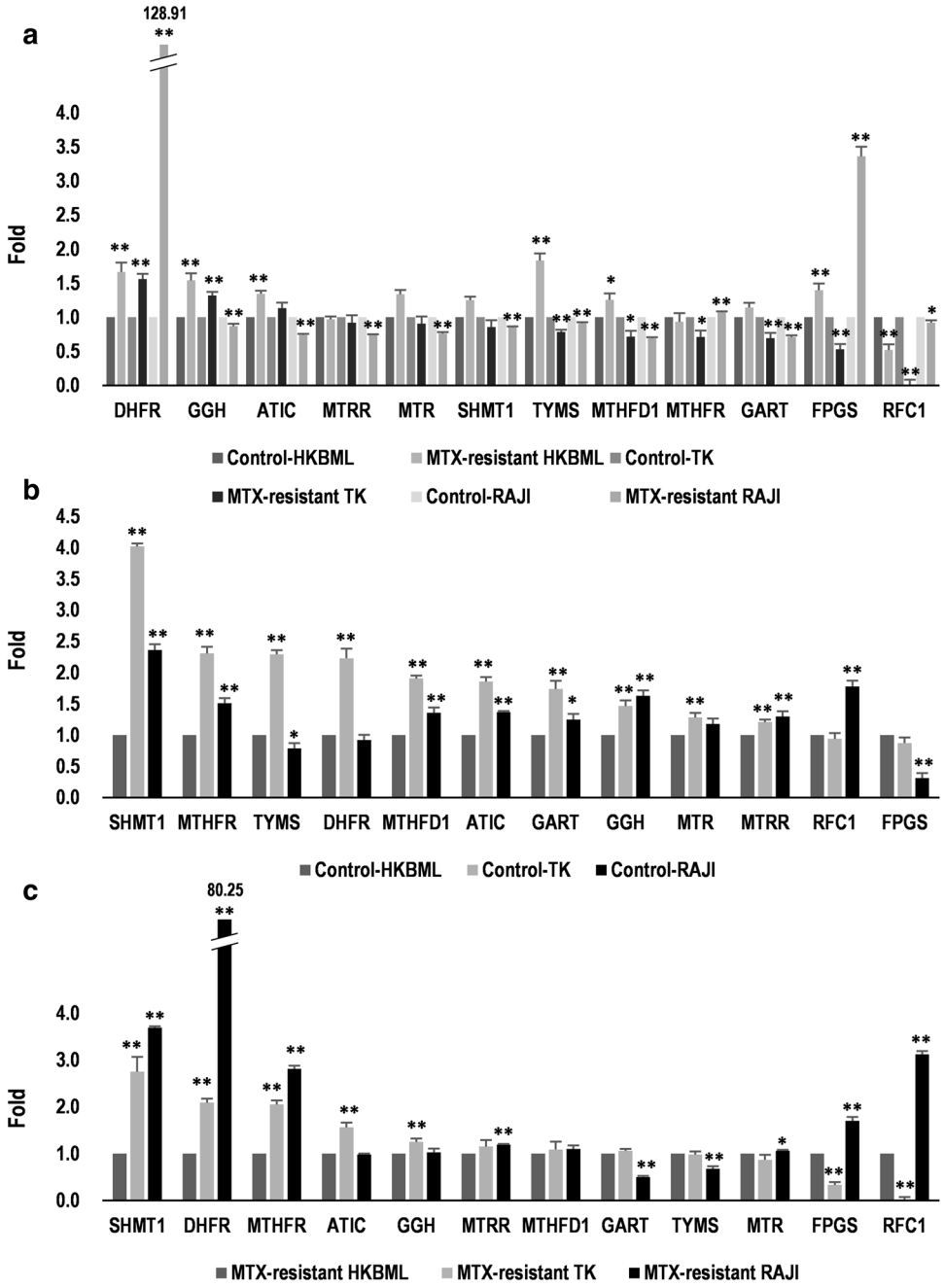

Fig. 2 Differential expression of the genes related to folate metabolism in the MTX-resistant cells. **a** Fold change in gene expression in the MTX-resistant cells compared with the corresponding control cells. **b**, **c** Fold changes of gene expression in the cell lines used. **b** Fold change in gene expression in TK and RAJI cells compared with HKBML cells. **c** Fold change in gene expression in the MTX-resistant TK and RAJI cells compared with the MTX-resistant HKBML cells. $^{**}P < 0.01$, $^{*}P < 0.05$

$P < 0.05$), compared to control RAJI (Fig. 2a). Basal expression levels of the genes, including MTHFR, TYMS, DHFR, MTHFD1, AITC, GART, and MTR, in RAJI were close to HKBML than those in TK (Fig. 2b). In contrast, the expression levels of SHMT1, DHFR, and MTHFR in MTX-RAJI were similar to MTX-TK than those in MTX-HKBML (Fig. 2c). Therefore, non-CNS lymphoma RAJI was different from CNS lymphomas HKBML and TK, such as differential expression of the almost genes related to MTX and folate metabolic pathway and changes of cell types between HKBML and TK according to their expression patterns, suggesting that the MTX and folate cycles were controlled by different manners in CNS lymphoma and non-CNS lymphoma.

Molecular target drug sensitivity in MTX-resistant cells

To determine the efficacy of molecular target drugs in the MTX-resistant cells, the cytotoxicity assay was performed. The resistance and/or sensitivity to molecular target drugs, including bortezomib (proteasome inhibitor), ibrutinib (Bruton's tyrosine kinase inhibitor), lenalidomide (immunomodulatory and antineoplastic agents), EPZ-6438 (also known

as Tazemetostat; histone methyltransferase EZH2 inhibitor), and azacytidine (also known as 5-AzaC; DNA methyltransferase inhibitor) of the cells were evaluated using the ratio of IC_{50} in MTX-resistant cells compared with that in the parent cells, after treatment with various concentrations of molecular target drugs for 48 h (Table 2, Fig. 3, and Supplementary Figure S1). MTX-HKBML acquired higher IC_{50} of bortezomib (4.4 nM), compared with control-HKBML (2.99 nM), indicating 1.46-fold resistance to bortezomib in MTX-HKBML (Fig. 3a and Table 2). Similarly, MTX-TK acquired lower IC_{50} of MTX (4.34 nM), compared with control-TK (13.52 nM), indicating 3.1-fold sensitivity to bortezomib in MTX-TK (Fig. 3b and Table 2). MTX-RAJI acquired lower IC_{50} of MTX (12.94 nM), compared with control-RAJI (19.45 nM), indicating 1.5-fold sensitivity to bortezomib in MTX-RAJI (Fig. 3c and Table 2). Thus, these cell lines were sensitive to bortezomib and MTX-TK exhibited improved sensitivity compared to the other two cell lines. In addition, EPZ-6438 and azacytidine also showed 1.26-fold and 2.47-fold sensitivities, respectively, in MTX-TK (Table 2, Fig. 3d, and Supplementary Figure S1h, k). These results suggest that the MTX-TK cell line acquired strong sensitivity to bortezomib, which is consistent with decreased expression of TYMS, MTHFD1, MTHFR, GART, and FPGS (Fig. 2a), resulting in dysregulated purine and pyrimidine syntheses and growth suppression. A conversion of the MTX metabolic pathway in MTX-TK may also be involved in an epigenetic regulation of the promoters of the genes related to MTX and folate cycles.

Combination of molecular target drugs on MTX

Furthermore, we demonstrated the combination of molecular target drugs on MTX and evaluated improved effects of MTX (Table 3 and Supplementary Figure S2). Drug combinations of bortezomib on MTX were very effective in MTX-HKBML, MTX-TK, and MTX-RAJI, which showed MTX sensitivities of 120.55-fold to MTX-HKBML, 3.44-fold to MTX-TK, and 4.42-fold to MTX-RAJI (Table 3 and Supplementary Figure S2a–c). In addition, ibrutinib on MTX showed MTX sensitivities of 80.99-fold to MTX-HKBML and 4.06-fold to MTX-RAJI (Table 3 and Supplementary Figure S2d, f). Azacytidine on MTX also showed MTX sensitivities of 19.09-fold to MTX-HKBML and 4.93-fold to MTX-RAJI (Table 3 and Supplementary Figure S2g, i). The CI values of MTX and other molecular target drugs, including bortezomib, ibrutinib, and azacytidine, were calculated in the MTX-resistant cells, as shown in Fig. 3e. The results returned synergistic effects of bortezomib on MTX in MTX-TK (CI 0.384), but not in MTX-HKBML and MTX-RAJI, suggesting that PCNSL-like TK or its acquisition mechanism of the MTX resistances is distinguished from

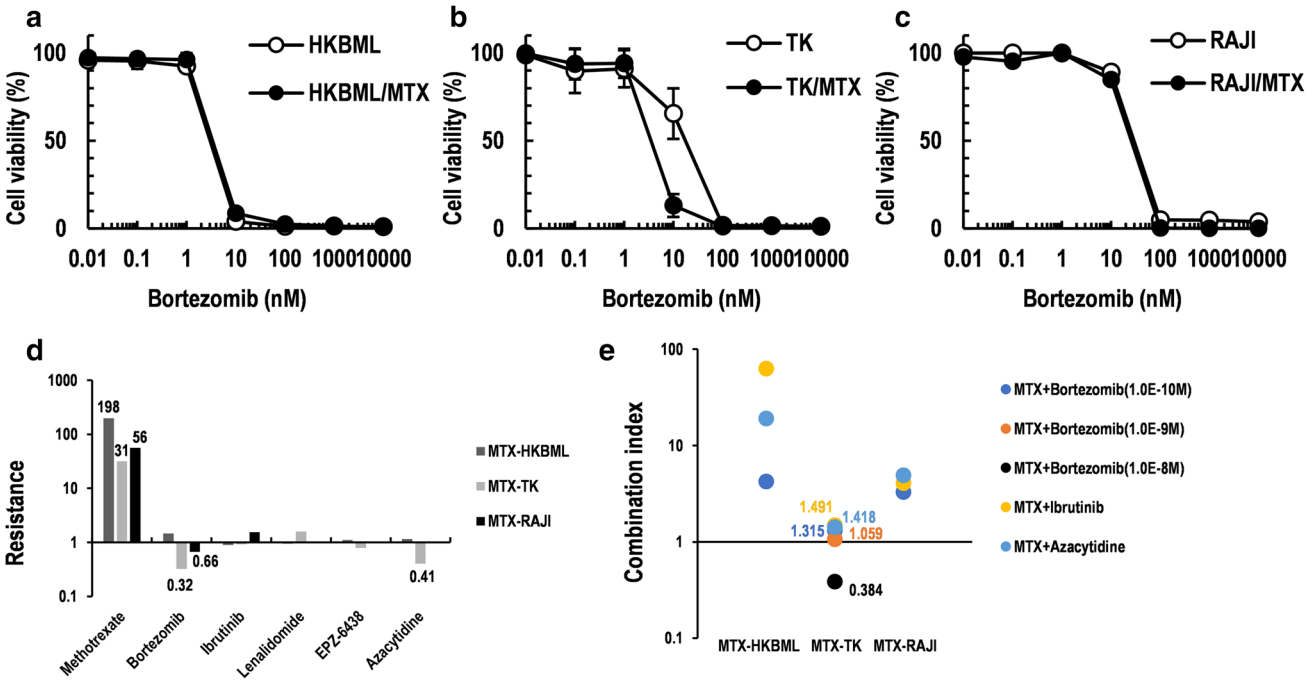

Fig. 3 Sensitivity of molecular target drugs in the MTX-resistant cells. **a**–**c** Sensitivity to bortezomib in the MTX-resistant HKBML (**a**), TK (**b**), and RAJI cells (**c**). Cell viabilities are shown. Open and closed circles indicate control and MTX-resistant cells. **d** Resistance to MTX and sensitivity of molecular target drugs in the MTX-resistant cells. **e** The combination index (CI) values of MTX and other molecular target drugs, including bortezomib, ibrutinib, and azacytidine in the MTX-resistant cells. CI < 1; synergism, CI 1; additive effect, CI > 1; antagonism

Table 3 The IC_{50} values of methotrexate in the MTX-resistant cells treated with molecular target drugs

Cells	Drugs	Concentration of additional drugs (M)	IC_{50} of MTX (μM)	Fold changes of IC_{50} of MTX
Control HKBML	MTX	–	0.845	1
MTX-resistant HKBML	MTX	–	167.88	198.674
MTX-resistant HKBML	MTX + bortezomib	1×10^{-9}	1.393	1.648
MTX-resistant HKBML	MTX + ibrutinib	1×10^{-8}	2.073	2.453
MTX-resistant HKBML	MTX + azacytidine	1×10^{-9}	8.795	10.408
Control TK	MTX	–	0.068	1
MTX-resistant TK	MTX	–	2.152	31.647
MTX-resistant TK	MTX + bortezomib	1×10^{-10}	1.587	23.338
MTX-resistant TK	MTX + bortezomib	1×10^{-9}	1.535	22.573
MTX-resistant TK	MTX + bortezomib	1×10^{-8}	0.626	9.205
MTX-resistant TK	MTX + ibrutinib	1×10^{-9}	1.39	20.441
MTX-resistant TK	MTX + ibrutinib	1×10^{-8}	1.434	21.088
MTX-resistant TK	MTX + azacytidine	1×10^{-9}	1.515	22.279
Control RAJI	MTX	–	0.043	1
MTX-resistant RAJI	MTX	–	2.426	56.418
MTX-resistant RAJI	MTX + bortezomib	1×10^{-9}	0.549	12.767
MTX-resistant RAJI	MTX + ibrutinib	1×10^{-8}	0.598	13.906
MTX-resistant RAJI	MTX + azacytidine	1×10^{-9}	0.492	11.441

IC_{50} 50% inhibitory concentration

PCNSL-like HKBML and non-PCNSL-like RAJI. These results suggest that bortezomib is compatible with MTX in MTX-resistant HKBML, TK, and RAJI. Further, ibrutinib and azacytidine on MTX are also effective to MTX-resistant HKBML and RAJI. Especially, synergistic effects of MTX and bortezomib were only observed in the MTX-TK. The mosaic combination of molecular target drugs on MTX against MTX-resistant CNS and non-CNS lymphoma should be further studied in detail.

Discussion

DHFR is a key enzyme inhibited competitively by MTX. TYMS generates deoxythymidylate monophosphate (dTMP) from deoxyuridylate monophosphate (dUMP) using 5,10-methylene-THF. Both GART and ATIC require 10-formyl-THF in purine synthesis [26]. Hence, these enzymes are also the key targets in the MTX metabolism [12]. Intracellular accumulation of long-chain MTX-PGs converted by FPGS enhances prolonged inhibition of DHFR [27, 28]. MTX-PGs also inhibit other enzymes involved in purine and pyrimidine syntheses, such as TYMS, ATIC, and GART [29, 30]. DHFR is a predominant target of MTX itself and MTX-PGs. Therefore, increased DHFR also has a pivotal role in MTX resistance [31, 32]. In cutaneous T-cell lymphoma cells, a heterogeneous group of NHLs involving the skin, combinational therapy with MTX and bortezomib induces apoptosis with altered gene expression in DNA repair pathway in vitro [33]. Twenty patients with mantle cell lymphoma (MCL) showed no pulmonary or neurological dose-limiting toxicity for bortezomib with R-Hyper-CVAD and R-M/A, indicating lack of toxicity for bortezomib-containing polychemotherapy [34]. In the phase 2 trial of bortezomib-containing polychemotherapy for 95 MCL patients, bortezomib provided a 33% response rate in relapsed/refractory MCL [35]. On the other hand, bortezomib is also known to target molecules downstream of interleukin-15 receptor signaling [36]. In large granular lymphocytic leukemia, rare lymphoproliferative disorders of transformed natural killer and T cells with chronic neutropenia lacking typical large granular lymphocytes of the blood, bortezomib fails to elicit a response, whereas a classical MTX regimen obtains partial remission [37]. Furthermore, double hit lymphoma cell lines for MYC proto-oncogene and B cell lymphoma 2 mutations, including Sc-1 and OcI-LY18, were sensitive to MTX, bortezomib, doxorubicin, and cytarabine [38]. Combinational chemotherapy using MTX and bortezomib can be used in clinical practice in several lymphomas. However, to date, there are no reports for MTX/bortezomib clinical trials and preclinical study in PCNSL. In general, many molecular target drugs are unable to exert therapeutic potentials against CNS disorders including lymphoma and glioma, because blood–brain barrier blocks their brain entry [39]. Bortezomib rarely penetrates a cerebrospinal fluid in pediatric relapsed/refractory acute lymphoblastic leukemia [40].

Intranasal delivery of bortezomib with perillyl alcohol prolongs survival of glioblastoma rat model [41]. P-Glycoprotein inhibition also enhances CNS uptake of bortezomib in spinal muscular atrophy [42]. Thus, if bortezomib is used for CNS lymphoma in preclinical studies and clinical trials, higher concentration than in vitro cell culture, or modified reagents for penetration to blood–brain barrier would be required.

In this study, we generated two MTX-resistant PCNSL cell lines, and one MTX-resistant Burkitt lymphoma cell line, as a non-CNS lymphoma reference. Of the three MTX-resistant cell lines, MTX-HKBML exhibited markedly strong resistance to MTX. Besides, increased expression of GGH and DHFR might lead to the accumulation of MTX and THF in both MTX-HKBML and MTX-TK (Fig. 4). In purine and pyrimidine syntheses, dysregulated expression of TYMS, FPGS, and MTHFD1 seemed to affect DNA synthesis in both MTX-HKBML and MTX-TK (Fig. 4). With respect to the MTX and folate metabolic pathway genes, expression analysis revealed their upregulation in MTX-HKBML and downregulation in MTX-TK, compared to the control cells (Fig. 4), which is consistent with the result from the bortezomib sensitivity in MTX-TK, but not in MTX-HKBML. These results suggest that there are different cell-type-specific changes in the metabolic pathways for MTX and folate, bortezomib sensitivity, and purine and pyrimidine syntheses in the MTX-resistant PCNSL cells, which should be further analyzed in future. While the expression of SLC19A1 (also known as RFC1) was decreased in the MTX-resistant cells (Fig. 4), MTX was incorporated and accumulated in the MTX-resistant cells. The reason why such contradiction was observed (e.g., protein expression, post-translational modification, and subcellular localization) should also be investigated in future studies. Meanwhile, TK, but not HKBML and RAJI, was flexible for sensitivities to molecular target drugs, including lenalidomide, EPZ-6438, and azacytidine. Also, MTX sensitivities were improved with drug combination of bortezomib, ibrutinib, and azacytidine. Furthermore, the CI value of MTX and bortezomib only indicated a synergy in the MTX-TK cells, suggesting a possibility of additional molecular target drugs on continuous MTX

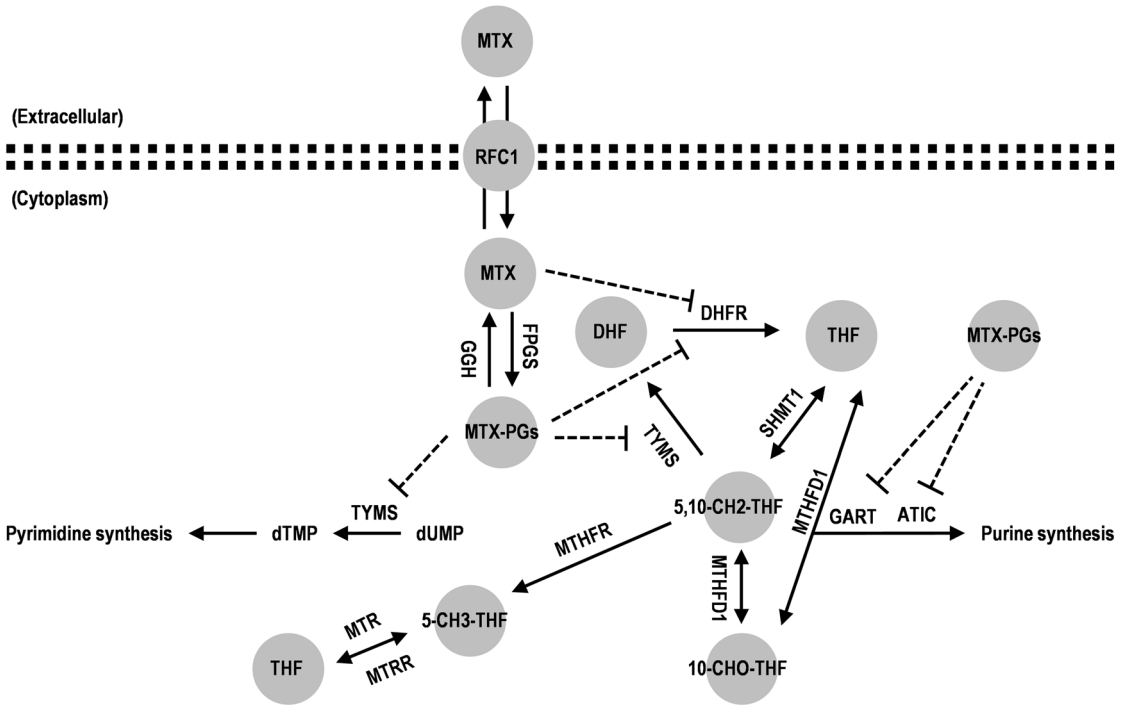

	DHFR	GGH	FPGS	MTHFR	GART	MTHFD1	ATIC	MTR	MTRR	SHMT1	TYMS	RFC1
MTX-resistant HKBML	+	+	+			+	+				+	-
MTX-resistant TK	+	+	-	-	-	-					-	-
MTX-resistant RAJI	+	-	+	+	-	-	-	-	-	-	-	-

Fig. 4 Cell-type-specific kinetics of MTX and folate metabolism in the MTX-resistant lymphoma cells. **a** Schematic representation of the MTX and folate metabolic pathways. Arrows and dotted lines denote enzymatic activity and inhibition, respectively. **b** Increased (+) and decreased (−) expression of the genes in the MTX-resistant cells is summarized

treatments for CNS lymphomas in clinical trials. Our data clearly demonstrated that bortezomib was effective for cell growth and maintenance of MTX-resistant HKBML, TK, and RAJI. However, cell-type specificities of improved sensitivities to MTX were considered among CNS and non-CNS lymphoma cells. This would be a hint to step toward animal experiments. These MTX-resistant lymphoma cell lines established may also be useful as in vitro relapse models for the development of MTX experimental medicine and of de novo salvage chemotherapy and drug discovery.

Acknowledgements The study was supported by the MEXT KAKENHI Grant numbers 16H05441, 16K10766, and 18K09001.

Author contributions AH and RY designed the experiments. AH and YT performed the experiments. AH, YT, and RY analyzed data. AH, YT, and RY wrote the manuscript.

Compliance with ethical standards

Conflict of interest The authors have declared that no conflict of financial and non-financial interest exists.

References

1. Panages KS, Elkin EB, DeAngelis LM et al (2005) Trends in survival from primary central nervous system lymphoma, 1975–1999: a population-based analysis. Cancer 104:2466–2472
2. Ricard D, Idbaih A, Ducray F et al (2012) Primary brain tumours in adults. Lancet 379:1984–1996
3. Louis DN, Perry A, Reifenberger G et al (2016) The 2016 World Health Organization classification of tumors of the central nervous system: a summary. Acta Neuropathol 131:803–820
4. Ferreri AJ, Reni M, Foppoli M et al (2009) High-dose cytarabine plus high-dose methotrexate versus high-dose methotrexate alone in patients with primary CNS lymphoma: a randomised phase 2 trial. Lancet 374:1512–1520
5. Thiel E, Korfel A, Martus P et al (2010) High-dose methotrexate with or without whole brain radiotherapy for primary CNS lymphoma (G-PCNSL-SG-1): a phase 3, randomised, non-inferiority trial. Lancet Oncol 11:1136–1147
6. Morris PG, Correa DD, Yahalom J et al (2013) Rituximab, methotrexate, procarbazine, and vincristine followed by consolidation reduced-dose whole-brain radiotherapy and cytarabine in newly diagnosed primary CNS lymphoma: final results and long-term outcome. J Clin Oncol 31:3971–3979
7. Reni M, Ferreri AJ, Villa E (1999) Second-line treatment for primary central nervous system lymphoma. Br J Cancer 9:530–534
8. Rushworth D, Mathews A, Alpert A et al (2015) Dihydrofolate reductase and thymidylate synthase transgenes resistant to methotrexate interact to permit novel transgene regulation. J Biol Chem 290:22970–22976
9. Mattaini KR, Sullivan MR, Vander Heiden MG (2016) The importance of serine metabolism in cancer. J Cell Biol 214:249–257
10. Gorlick R, Goker E, Trippett T et al (1996) Intrinsic and acquired resistance to methotrexate in acute leukemia. N Engl J Med 335:1041–1048
11. Zhao R, Goldman ID (2003) Resistance to antifolates. Oncogene 22(47):7431–7457
12. Walling J (2006) From methotrexate to pemetrexed and beyond. A review of the pharmacodynamic and clinical properties of antifolates. Investig New Drugs 24:37–77
13. Jin G, Huang J, Hu Z et al (2010) Genetic variants in one-carbon metabolism-related genes contribute to NSCLC prognosis in a Chinese population. Cancer 116:5700–5709
14. Davis RE, Brown KD, Siebenlist U et al (2001) Constitutive nuclear factor kappaB activity is required for survival of activated B cell-like diffuse large B cell lymphoma cells. J Exp Med 194:1861–1874
15. Strauss SJ, Higginbottom K, Jüliger S et al (2007) The proteasome inhibitor bortezomib acts independently of p53 and induces cell death via apoptosis and mitotic catastrophe in B-cell lymphoma cell lines. Cancer Res 67:2783–2790
16. Odqvist L, Montes-Moreno S, Sánchez-Pacheco RE et al (2014) NFkappaB expression is a feature of both activated B-cell-like and germinal center B-cell-like subtypes of diffuse large B-cell lymphoma. Mod Pathol 27:1331–1337
17. Richardson PG, Barlogie B, Berenson J et al (2003) A phase 2 study of bortezomib in relapsed, refractory myeloma. N Engl J Med 348:2609–2617
18. Fisher RI, Bernstein SH, Kahl BS et al (2006) Multicenter phase II study of bortezomib in patients with relapsed or refractory mantle cell lymphoma. J Clin Oncol 24:4867–4874
19. Dunleavy K, Pittaluga S, Czuczman MS et al (2009) Differential efficacy of bortezomib plus chemotherapy within molecular subtypes of diffuse large B-cell lymphoma. Blood 113:6069–6076
20. Ribrag V, Gisselbrecht C, Haioun C et al (2009) Efficacy and toxicity of 2 schedules of frontline rituximab plus cyclophosphamide, doxorubicin, vincristine, and prednisone plus bortezomib in patients with B-cell lymphoma: a randomized phase 2 trial from the French Adult Lymphoma Study Group (GELA). Cancer 115:4540–4546
21. Ruan J, Martin P, Furman RR et al (2011) Bortezomib plus CHOP-rituximab for previously untreated diffuse large B-cell lymphoma and mantle cell lymphoma. J Clin Oncol 29:690–697
22. Offner F, Samoilova O, Osmanov E et al (2015) Frontline rituximab, cyclophosphamide, doxorubicin, and prednisone with bortezomib (VR-CAP) or vincristine (R-CHOP) for non-GCB DLBCL. Blood 126:1893–1901
23. Leonard JP, Kolibaba KS, Reeves JA et al (2017) Randomized phase II study of R-CHOP with or without bortezomib in previously untreated patients with non-germinal center B-cell-like diffuse large B-cell lymphoma. J Clin Oncol 35:3538–3546
24. Huang L, Jiang Y, Chen Y (2017) Predicting drug combination index and simulating the network-regulation dynamics by mathematical modeling of drug-targeted EGFR-ERK signaling pathway. Sci Rep 7:40752
25. Livak KJ, Schmittgen TD (2001) Analysis of relative gene expression data using real-time quantitative PCR and the 2(-Delta Delta C(T)) method. Methods 25:402–408
26. Connelly S, DeMartino JK, Boger DL et al (2013) Biological and structural evaluation of 10*R*- and 10*S*-methylthio-DDACTHF reveals a new role for sulfur in inhibition of glycinamide ribonucleotide transformylase. Biochemistry 52:5133–5144
27. Bleyer WA (1977) Methotrexate: clinical pharmacology, current status and therapeutic guidelines. Cancer Treat Rev 4:87–101
28. Jolivet J, Cowan H, Curt A et al (1983) The pharmacology and clinical use of methotrexate. N Engl J Med 309:1094–1104
29. Allegra CJ, Chabner BA, Drake JC et al (1985) Enhanced inhibition of thymidylate synthase by methotrexate polyglutamates. J Biol Chem 260:9720–9726

30. Chabner BA, Allegra CJ, Curt GA et al (1985) Polyglutamation of methotrexate. Is methotrexate a prodrug? J Clin Investig 76:907–912
31. Göker E, Kheradpour A, Waltham M et al (1995) Acute monocytic leukemia: a myeloid leukemia subset that may be sensitive to methotrexate. Leukemia 9:274–276
32. Matherly LH, Taub JW, Ravindranath Y et al (1995) Elevated dihydrofolate reductase and impaired methotrexate transport as elements in methotrexate resistance in childhood acute lymphoblastic leukemia. Blood 85:500–509
33. Mpakou V, Papadavid E, Kontsioti F et al (2017) Apoptosis induction and gene expression profile alterations of cutaneous T-cell lymphoma cells following their exposure to bortezomib and methotrexate. PLoS One 12:e0170186
34. Romaguera JE, Fayad LE, McLaughlin P et al (2010) Phase I trial of bortezomib in combination with rituximab-HyperCVAD alternating with rituximab, methotrexate and cytarabine for untreated aggressive mantle cell lymphoma. Br J Haematol 151:47–53
35. Romaguera JE, Wang M, Feng L et al (2018) Phase 2 trial of bortezomib in combination with rituximab plus hyperfractionated cyclophosphamide, vincristine, doxorubicin, and dexamethasone alternating with bortezomib, rituximab, methotrexate, and cytarabine for untreated mantle cell lymphoma. Cancer 124:2561–2569
36. Hodge DL, Yang J, Buschman MD et al (2009) Interleukin-15 enhances proteasomal degradation of bid in normal lymphocytes: implications for large granular lymphocyte leukemias. Cancer Res 69:3986–3994
37. Bagacean C, Tempescul A, Patiu M et al (2016) Atypical aleukemic presentation of large granular lymphocytic leukemia: a case report. OncoTargets Ther 10:31–34
38. Johnson-Farley N, Veliz J, Bhagavathi S et al (2015) ABT-199, a BH3 mimetic that specifically targets Bcl-2, enhances the antitumor activity of chemotherapy, bortezomib and JQ1 in "double hit" lymphoma cells. Leuk Lymphoma 56:2146–2152
39. Gozzetti A, Cerase A (2014) Novel agents in CNS myeloma treatment. Cent Nerv Syst Agents Med Chem 14:23–27
40. Kaspers GJL, Niewerth D, Wilhelm BAJ et al (2018) An effective modestly intensive re-induction regimen with bortezomib in relapsed or refractory paediatric acute lymphoblastic leukaemia. Br J Haematol 181:523–527
41. Wang W, Swenson S, Cho HY et al (2019) Efficient brain targeting and therapeutic intracranial activity of bortezomib through intranasal co-delivery with NEO100 in rodent glioblastoma models. J Neurosurg 15:1–9
42. Foran E, Kwon DY, Nofziger JH et al (2016) CNS uptake of bortezomib is enhanced by P-glycoprotein inhibition: implications for spinal muscular atrophy. Neurobiol Dis 88:118–124